CHARGE DENSITY DISTRIBUTIONS, MOMENTUM DENSITY DISTRIBUTIONS, AND ELASTIC FORM FACTORS OF EXOTIC ONE- AND TWO-PROTON HALO NUCLEI

Maha Taha Yaseen*, Akram M. Ali

Physics Department, College of Science, University of Anbar, Anbar, Iraq

Corresponding author: mahaalabraheem@gmail.com

Received: 14 March 2020 Revised and Accepted: 8 July 2020

Abstract

In this article, a comprehensive study concerning one- and two- proton halo nuclei is presented. The theoretical and experimental nucleon density distributions (NDD), nucleon momentum distributions (NMD) and elastic electron scattering from factors of ^{23}Al, ^{26}P, and ^{28}S using Coherent Density Fluctuation Model (CDFM) and 2pF approach are elaborated. In detail, a long-tail phenomenon was attained within the NDD and NMD investigations which considered a distinguishable property of proton halo nuclei. In the form factors profiles, the mass center, $F_{cm}(q)$, is applied in order to convert the attained form factors into an appropriate analytical representation. Additionally, the nuclei under consideration were compared to their stable forms (^{27}Al, ^{31}P, and ^{32}S) in term of NDD and form factors profiles. The proposed study demonstrates a new approach for an accurate evaluation of the aforementioned nuclear quantities.

1. Introduction

The structural investigations of a nuclei located at a certain distance from the β stability line is of great importance in the field of nuclear physics. Herein, quality measures have been reported to elaborate more on the addressed matter; a perfect example of this is the discovery of halo phenomena in the exotic nuclei [1]. In detail, a halo nucleus possesses a specific proton/neutron excess in which a particular number of nucleons are inadequately bounded to the system [2, 3]. Accordingly, such a halo system is thoroughly elucidated through the few-body model by which a core and its outside nucleons are taken into considerations. Due to the significance of several quantities in the halo phenomena, such as nucleon density distributions (NDD), nucleon momentum distributions (NMD) and form factors, a number of approaches have been proposed throughout the past few decades to explore the addressed quantities of such phenomena in particular locations placed far from the β stability line [4-8]. However, further examinations on the existed models are needed combined with experimental investigations to faultlessly illustrate the discussed structure.

The mean field model was used to evaluate the form factors, NDD and cross-section of ^{28}S and ^{12}O; whereby it was evidently proven that the charge density of the last protons has a direct correlation to the form factors and cross-section values [4]. The longitudinal and transverse elastic electron scattering form factors of ^{8}B nuclei were investigated via the large space shell model; thereby the presence of proton halo resulted in significant change in the form factors behavior [5]. The three-body as well as the realistic two-body models were employed to investigate some nuclear quantities of ^{18}Ne and ^{28}S. Specifically, the three-body model was found to be proper to elaborate more on proton-rich nuclei as comparted to the realistic two-body model [6]. Another research group reported the calculation of NDD and form factors for some proton-rich nuclei (^{27}P, ^{23}Al, ^{17}Ne, ^{17}F, and ^{8}B) using the wave function of Wood-Saxon model. They concluded that the existence of the halo structure can be evidenced via the observation of the long-tail behavior [7]. K. Santhosh and I. Sukumaran investigated the existing possibility of one proton halo (^{8}B, ^{12}N, ^{13}N, ^{17}F) and two halo nuclei (^{9}C, ^{17}Ne, ^{18}Ne, ^{20}Mg) using Coulomb and proximity potential model (CPPM). It was reported that there is higher probability of one proton halo emission nuclei as compared to those of two proton halo nuclei [8].

In this attempt, this study reports a theoretical and experimental evaluations of NDD, NMD, and form factors for exotic one proton halo nuclei (^{23}Al, ^{26}P) and two proton halo nuclei (^{28}S). Particularly, the NDD was calculated using shell model, while the NMD was evaluated using CDFM. Furthermore, the long-tail performance was observed when $q \geq 2$ within the NDD profile.

2. Theory

A nuclei NDD of single body operator can be expressed using the following relation [9]:

$$\rho(r) = \frac{1}{4\pi} \sum_{n\ell} \xi_{n\ell}\, 4(2\ell + 1) \emptyset^*_{nl}(r) \emptyset_{nl}(r) \tag{1}$$

In Equation (1), the term $\xi_{n\ell}$ represents the probability of the nucleon occupation ($\xi_{n\ell} = 0 < \xi_{n\ell} < 1$ for open shell nuclei and 0 or 1 for closed shell nuclei), while the wave function radial part of the single particle harmonic oscillator is represented by the term $\emptyset_{nl}(r)$. The NDDs of the selected nuclei (^{23}Al, ^{26}P and ^{28}S) located at the end of the shell are derived on the basis that there is a core, ^{22}Mg, ^{25}Si and ^{26}Si in our case. These cores are of filled $1s$ and $1d$ shells, whilst the nucleons occupation number in $2S$ as well as $1d$ shells are equal to $A - \alpha_1$ and $A - 20 + \alpha_1$, respectively. Therefore, the term $\rho(r)$ in Equation (1) can be further simplified as demonstrated in Equation (2).

$$(r) = \frac{exp(-R^2/b^2)}{\pi^{3/2} b^3} \left\{10 - \frac{3}{2}\alpha_1 + 2\alpha_1 (\frac{r}{b})^2 + \left[\frac{4A}{15} - \frac{8}{3} - \frac{2\alpha_1}{5}\right] (\frac{r}{b})^4\right\} \tag{2}$$

where parameter α_1 signifies the nucleon occupation number's deviation with the assumption of simple shell model ($\alpha_1 = 0$), while the nuclear mass number and the harmonic oscillator size are represented by parameters A and b.

The NDD normalized condition is then expressed as follow [10]:

$$A = 4\pi \int_0^\infty \rho(r) r^2 dr \tag{3}$$

The sd-shell nuclei NMD is evaluated on the basis of shell model employing the wave function of the single particle harmonic oscillator with respect to the momentum representations [11]. The NMD can be obtained using Equation (4).

$$n(k) = \frac{b^3}{\pi^{3/2}} \exp\left(-\frac{b^2}{k^2}\right) \left(4 + 8(bk)^4 + \frac{4(A-40)}{15} (bk)^6\right) \tag{4}$$

In the framework of CDFM [12, 13], the mixed density can be expressed as:

$$\rho(r, r') = \int_0^\infty |f(x)|^2 \rho_x(r, r') dr \tag{5}$$

$$\rho_x(r, r') = 3\rho_0(x) \frac{j_1(k_{F(x)}|r - r'|)}{k_F(x)|r - r'|} \theta\left(x - \frac{1}{2}|r - r'|\right) \tag{6}$$

The term $\rho_x(r, r')$ is the mixed density, CDFM framework, for A nucleons which is uniformly distributed alongside a radius of x as well as density given by the following equation:

$$\rho_0(x) = 3A/4\pi x^3 \tag{7}$$

Hence, the Femi momentum is expressed as:

$$k_F(x) = (\frac{3\pi^2}{2} \rho_0(x))^{1/3} = (\frac{9\pi A}{8})^{1/3} \frac{1}{x} = \frac{\alpha}{x} \tag{8}$$

and θ as a step function can be given as:

$$\theta(y) = \begin{cases} 1, & y \geq 0 \\ 0, & y < 0 \end{cases} \tag{9}$$

Equation (5) is related to general statement in the CDFM framework that the nuclear matter NDD fluctuates around the averaged distribution; this particular instance maintains uniformity and spherical symmetry. Subsequently, In Equation (5), the diagonal element provides the single-particle density as represented in Equation (10).

$$\rho(r) = \rho_x(r, r' = r) \int_0^\infty |f(x)|^2 \rho_x(r) dx \quad (10)$$

The terms $\rho(r)$ as well as $f(x)|^2$, In Equation (10), can be represented using Equations (11) and (12), respectively.

$$\rho_x(r) = \rho_0(r)\theta(x - |\vec{r}|) \quad (11)$$

$$|f(x)|^2 = \frac{-1}{\rho_0(x)} \frac{d\rho(r)}{dr} \quad (12)$$

In Equation (10), the wave function $|f(x)|^2$ is evaluated in term of NDD where the normalization conditions are satisfied $(\int_0^\infty |f(x)|^2 = 1)$.

Hereinafter, the NMD can be expressed on the basis of Equation (10) as follow [14]:

$$n(k) = \int_0^\infty |f(x)|^2 n_x(k) dx \quad (13)$$

herein $n_x(k)$ is the system Fermi-momentum distribution with density of $\rho_o(x)$; and can be given as:

$$n_x(k) = \frac{4}{3}\pi x^3 \theta(k_F(x) - |k|) \quad (14)$$

Continuously, the term $n(k)$ can be given in term of $\rho_o(r)$ as:

$$n_{CDFM}(k) = (\frac{4\pi}{3})^2 \frac{4}{A}\left[6\int_0^{\alpha/k} \rho(x) x^5 dx - (\frac{\alpha}{k})^6 \rho(\frac{\alpha}{k})\right] \quad (15)$$

with the normalized condition $(A = \int n_{CDFM}(k) \frac{d^3k}{(2\pi)^3})$

In the CDFM framework, the form factor $(F(q))$ is also expressed [13]:

$$(q) = \frac{1}{A}\int |f(x)|^2 F(q, x) dx \quad (16)$$

$$F(q, x) = \frac{3A}{(qx)^2}\left[\frac{\sin(qx)}{(qx)} - \cos(qx)\right] \quad (17)$$

Equation (17) must be multiplied by a correction of free nucleon finite-size form factor (same protons and neutrons) and center of mass form factor [15]. This eliminates the false state appears from the indication of the mass center. These form corrections can be expressed as follow:

$$F_{fs}(q) = \exp\left(\frac{-0.43q^2}{A}\right) and\ F_{cm}(q) = \exp\left(\frac{b^2q^2}{4A}\right) \quad (18)$$

It is worth mentioning that the physical quantities discussed earlier are in the CDFM framework and expressed on the basis of weight function. Thus, it is worth trying to attain the weight function using theoretical considerations.

If Equation (2) inserted into the equation of weight function (12), an analytical expression cab be acquired as:

$$|f(x)|^2_{2pF} = \frac{8\pi x^4 \rho(x)}{3Ab^2} - \frac{16x^4}{3A\pi^{1/2}b^5}\left\{\left[\alpha_1 + (\frac{14A}{15} - \frac{8}{3} - \frac{\alpha_1}{5}\right](\frac{x}{b})^2\right\} exp\left(\frac{-x^2}{b^2}\right) \quad (19)$$

3. Results and discussion

The CDFM approach is presented in this study in order to investigate the ground state charge density and the associated root mean square (RMS) radii, NDD, NMD, and form factors. This is accomplished in connection with 2pF model. The aforementioned parameters are considered for one proton halo, ^{23}Al $(S_p = 0.141\, MeV, \tau_{1/2} = 470\, ms)$, ^{26}P $(S_p = 0.140\, MeV, \tau_{1/2} = 43.7\, ms)$. In particular, the nucleus ^{23}Al $(J^\pi, T = (5/2)^+, 3/2)$ is shaped by coupling the core ^{22}Mg $(J^\pi, T = (0)^+, 1)$ alongside one valence proton; and the nucleus ^{26}P $(J^\pi, T = (3)^+, 2)$ is formed by coupling the core ^{25}Si $(J^\pi, T = (5/2)^+, 3/2)$ with one valence proton. While, the nucleus ^{28}S $(S_{2p} = 3.36\, MeV, \tau_{1/2} = 125\, ms), (J^\pi, T = (0)^+, 0)$, which is two proton halo nucleus is formed by coupling the core ^{26}Si

$(J^{\pi}, T = (0)^{+}, 0)$ with two valence protons [16]. Continuously, the configuration of ^{22}Mg, ^{25}Si, and ^{26}Si are assumed as $1d\ (5/2)^{6}$, $1d\ (5/2)^{8}$, and $1d\ (5/2)^{10}$, respectively.

The evaluated neutron and proton charge RMS radii as well as the per nucleon binding energy for ^{23}Al, ^{26}P, and ^{28}S are tabulated in Table 1 alongside with the corresponding experimental data; these parameters were obtained using CDFM approach. As such, it can be noticed that the attained results are in an upright agreement with the experimental data for all mentioned nuclei.

Nuclei	$< r_p^2 >^{1/2}$	$< r_p^2 >_{exp}^{1/2}$	$< r_n^2 >^{1/2}$	$< r_n^2 >_{exp}^{1/2}$	Δr
^{23}Al	2.704	2.85 [17]	2.821	2.657	0.117
^{26}P	2.836	3.13 [18]	2.885	2.82	0.049
^{28}S	2.907	3.14 [19]	2.944	3.011	0.037

Table 1: Calculated proton and neutron RMS radii along with experiment results.

Table 2: Calculated matter RMS radii and binding energy per nucleon along with experimental result.

Nuclei	$< r_m^2 >^{1/2}$	$< r_m^2 >_{exp}^{1/2}$	BE (MeV)	BE_{exp} (MeV)
^{23}Al	2.907	2.905 [17]	7.335	7.336 [16]
^{26}P	3.029	3.00 [18]	7.187	7.198 [16]
^{28}S	3.104	3.27 [19]	7.472	7.479 [16]

Simultaneously, Figure 1 (a, and b) illustrates the theoretical and experimental values of the NDD for the selected nuclei alongside their cores using shell/2pF mathematical representations, respectively. Additionally, the theoretical and experimental NDD profile in the stated figure is varied because of the wave functions dissimilarities in shell and 2pF models, respectively. This particular observation is mainly attributed to the one valence proton of ^{23}Al and ^{26}P and two valence protons of ^{28}S in the halo orbits [20]. Fascinatingly, the experimental curves, Figure 1, exhibited the long-tail feature, which is a remarkable property of the proton halo nuclei; such a behavior is related to the presence of the outer one/two proton in the outer orbit [3]. While, the steep slope behavior was noticed in the theoretical curves. Concurrently, in accordance with Equation (2), it is obviously observed that the introduced nuclei depend directly on the mass number whereby ^{28}S nucleus possesses relatively larger mass number as compared to ^{26}P and ^{28}S., inset into Figure 1(a).

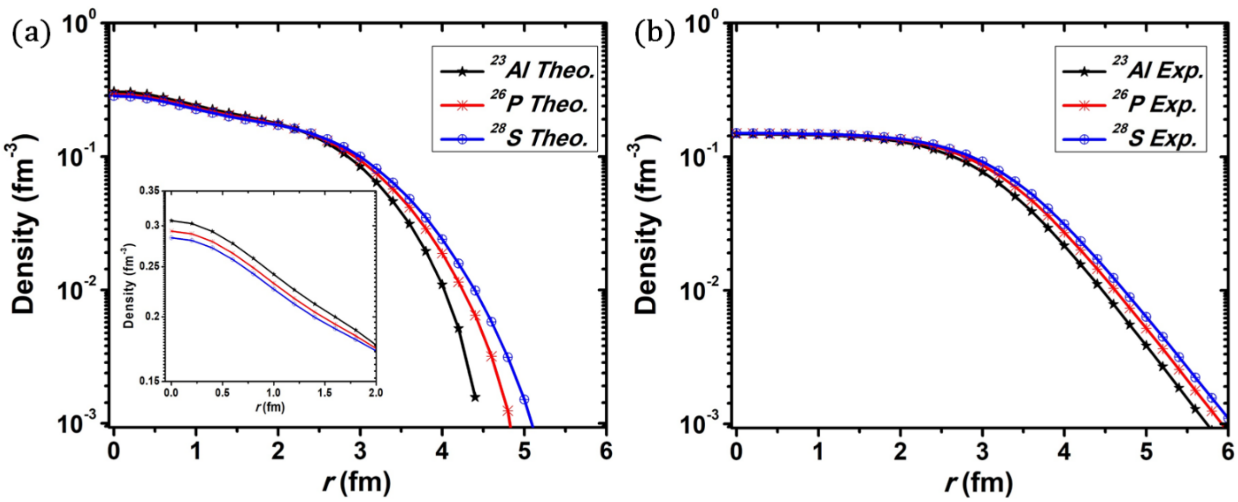

Figure 1: (a) experimental and (b) theoretical results of the NDD for exotic one- and two- proton halo.

Figure 2 presents a comparison of the calculated NDD outcomes of the exotic nuclei (^{23}Al, ^{26}P, and ^{28}S) with their stable forms (^{27}Al, ^{31}P, and ^{32}S). It can be clearly observed that the NDD of both exotic and stable nuclei are divers. Furthermore, the stable nuclei long-tail behavior in the experimental results (Figure 2 b, c, and d) was found to be longer than those of the exotic nuclei. This can be mainly attributed to the weak proton halo bound of the exotic nuclei (^{23}Al, ^{26}P, and ^{28}S) as compared to their stable form (^{27}Al, ^{31}P, and ^{32}S). This suggests that the halo phenomenon is associated with the outer one/two protons; thereby such a phenomenon is not linked to the core nucleons.

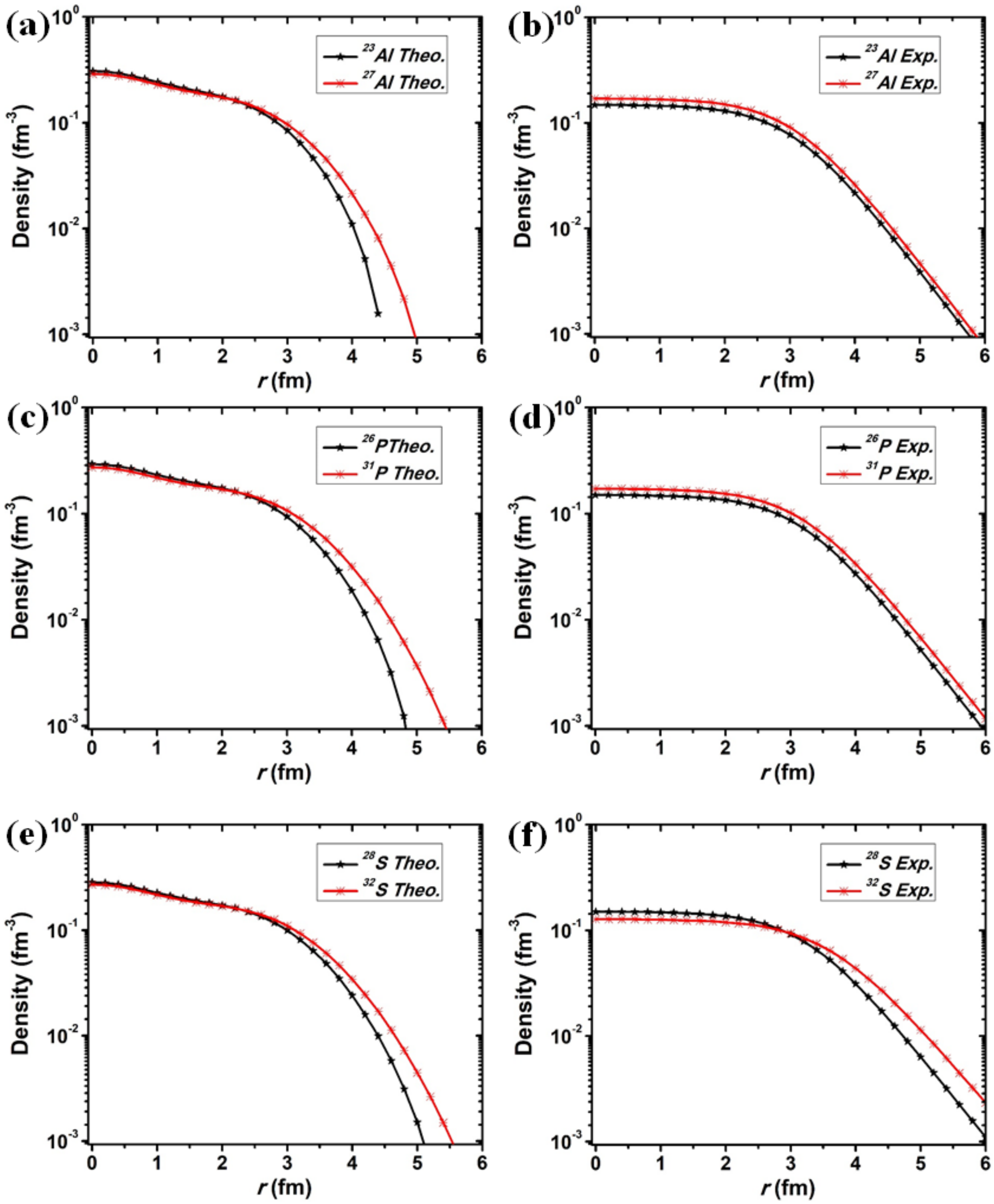

Figure 2: The theoretical and experimental nucleon density distribution of both stable and unstable nuclei: (a) theoretical ^{23}Al and ^{27}Al, (b) experimental ^{23}Al and ^{27}Al, (c) theoretical ^{26}P and ^{31}P, (d) experimental ^{26}P and ^{31}P, (e) theoretical 28S and 32S, and (f) experimental ^{28}S and ^{32}S.

ISSN- 2394-5125 VOL 7, ISSUE 15, 2020

The NMD of the introduced nuclei alongside their cores are elucidated as a function of the momentum $k(fm^{-1})$ in Figure 3; whereby both theoretical and experimental results are demonstrated using shell model and CDFM, respectively. Generally, the demonstrated results in Figure 3 showed similar behavior at high momentum region $(k \geq 1\, fm^{-1})$. However, the theoretical values revealed higher values than those obtained experimentally. Concurrently, at momentum regions where the value of k is less than 1, the curves obtained presented slight differences. Additionally, the long-tail behavior was observed at high momentum regions for both theoretical and experimental outcomes, including nuclei and their cores. This particular observation is in an upright agreement with those of NDD results (Figure 1). The findings suggest that the fluctuation function, $|f(x)|^2$, is relatively insignificant through Equation (19).

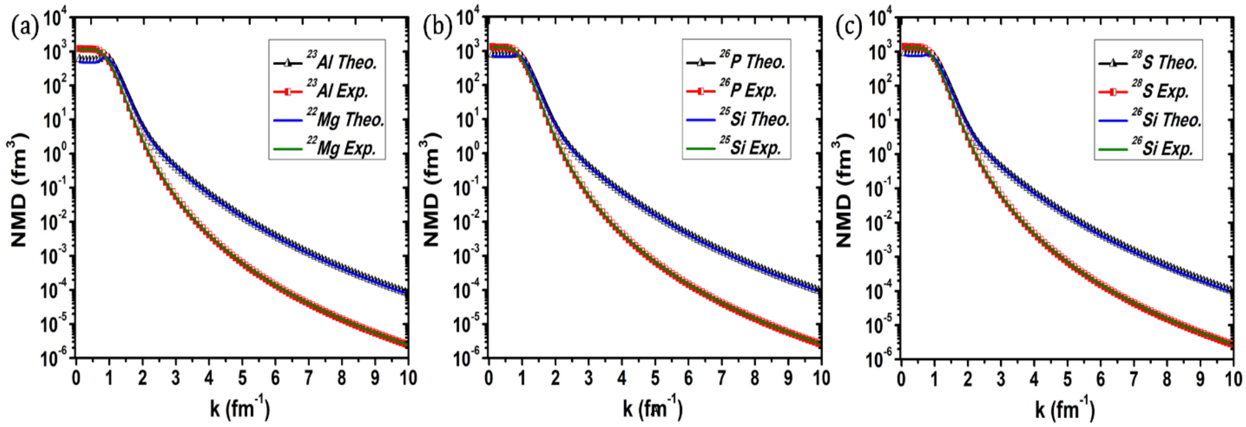

Figure 3: Theoretical and experimental NDM of ^{23}Al, ^{26}P, and ^{28}S and their cores (^{22}Mg, ^{25}Si, and ^{26}Si).

Figure 4 shows the form factors, experimental, with corrections and without corrections, of the employed nuclei and their cores. The ground state proton form factors, in Figure 4, are attained using Fourier-Bessel approach. In this investigation, plane wave Born approximation (PWBA) is used to study the incident/scattered electrons within the nuclei and their cores under consideration [20]. Consequently, a number of correction ought to be utilized in order to convert the attained form factors into an appropriate analytical representation; by which a comparison with the acquired experimental data can be elaborated. Hence, the mass center, $F_{cm}(q)$, is employed. This particular approach omits any false states occurred within the shell model mass center motion, announced in Equation (18) [15]. As shown in Figure 4, the obtained curves, including the three forms, are in a well-agreement, in which the demonstrated form factor agrees well with the experimental data. Moreover, Figure 5 illustrates a comparison concerning the corrected form factors of the exotic nuclei and their stable forms. The major alteration between the exotic nuclei and their stable forms could be attributed to the influence of the last proton density distribution as well as the differences obtained in the mass number and parameter b (1.802, 1.830, and 1.848 for ^{23}Al, ^{26}P, and ^{28}S, respectively). The b parameters for the cores ^{22}Mg, ^{25}Si, ^{26}Si are 1.792, 1.821, and 1.830, respectively.

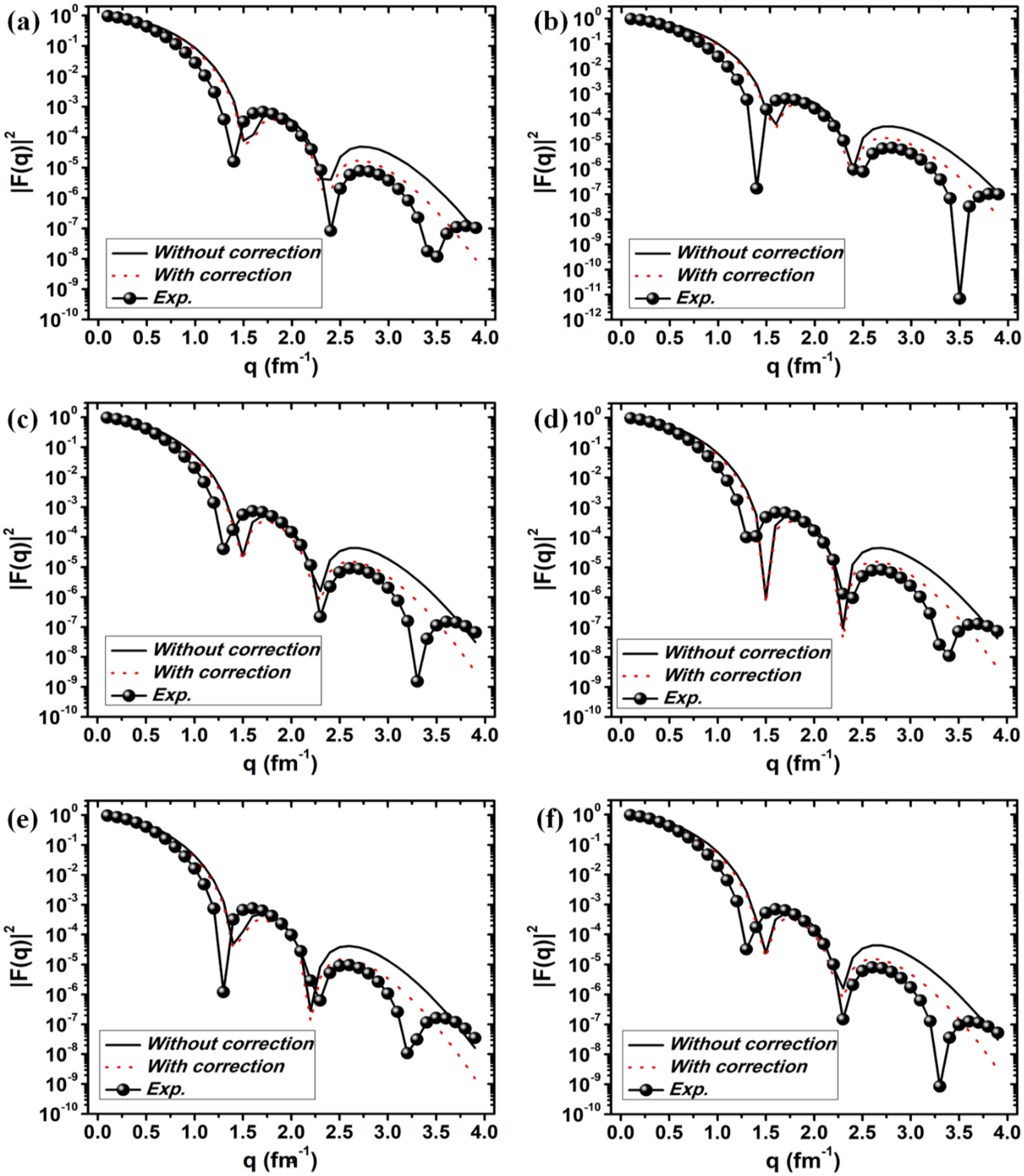

Figure 4: Experimental form factors alongside “with and without correction” of (a) ^{23}Al, (b) ^{22}Mg, (c) ^{26}P, (d) ^{25}Si, (e) ^{28}S, and (f) ^{26}Si.

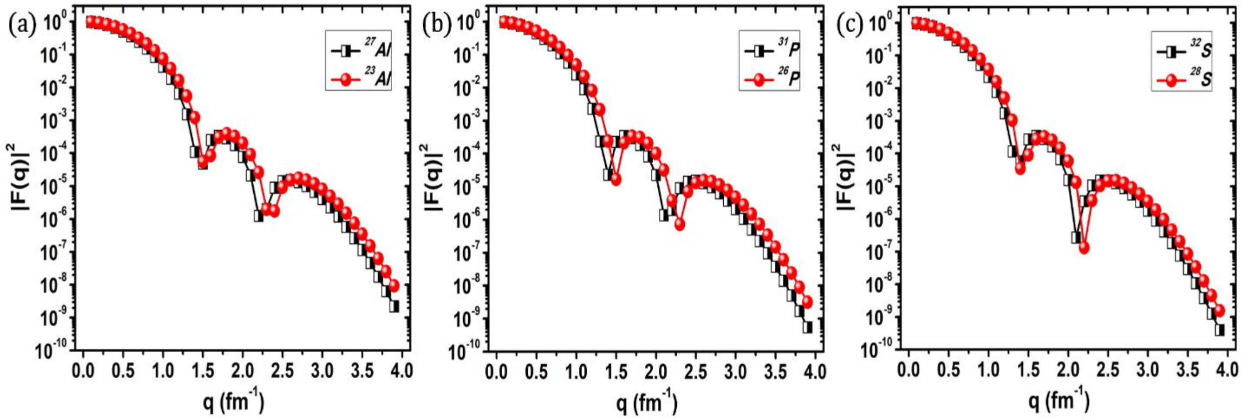

Figure 5: Comparison of unstable and stable nuclei: (a) ^{23}Al and ^{27}Al, (b) ^{26}P and ^{31}P, and (c) ^{28}S and ^{32}S.

Conclusion

The theoretical and experimental NDD, NMD and from factors concerning ^{23}Al, ^{26}P, and ^{28}S using Coherent CDFM and 2pF approaches were successfully particularized. The calculated RMS radii of the considered nuclei were compared to the experimental data published in previous reports. The long-tail feature of the proton halo nuclei within the NDD and NMD profiles was elucidated. Furthermore, the form factors attained results were corrected using $F_{cm}(q)$ method. Finally, a diverse behavior within the comparison between the exotic and stable utilized nuclei was observed for the NDD and NMD outcomes.

References

[1] I. Tanihata, H. Hamagaki, O. Hashimoto, S. Nagamiya, Y. Shida, N. Yoshikawa, O. Yamakawa, K. Sugimoto, T. Kobayashi, D. Greiner, Measurements of interaction cross sections and radii of He isotopes, Physics Letters B, 160 (1985) 380-384.

[2] G. Wen-Jun, J. Huan-Qing, L. Jian-Ye, Z. Wei, R. Zhong-Zhou, L. Xi-Guo, Total nuclear reaction cross section induced by halo nuclei and stable nuclei, Communications in Theoretical Physics, 40 (2003) 577.

[3] A.N. Abdullah, Matter density distributions and elastic form factors of some two-neutron halo nuclei, Pramana, 89 (2017) 43.

[4] Z. Wang, Z. Ren, Elastic electron scattering on exotic light proton-rich nuclei, Physical Review C, 70 (2004) 034303.

[5] S. Karataglidis, K. Amos, Electron scattering form factors from exotic nuclei, Physics Letters B, 650 (2007) 148-151.

[6] Y. Chu, Z. Ren, C. Xu, Properties of proton-rich nuclei in a three-body model, The European Physical Journal A, 37 (2008) 361-366.

[7] R.I. Noori, A.R. Ridha, Density Distributions and Elastic Electron Scattering Form Factors of Proton-rich 8B, 17F, 17Ne, 23Al and 27P Nuclei, Iraqi Journal of Science, (2019) 1286-1296.

[8] K. Santhosh, I. Sukumaran, Decay of $$ Z= 82 {-} 102$$ heavy nuclei via emission of one-proton and two-proton halo nuclei, Pramana, 92 (2019) 6.

[9] C.C. Moustakidis, S. Massen, One-body density matrix and momentum distribution in s− p and s− d shell nuclei, Physical Review C, 62 (2000) 034318.

[10] W.J. Thompson, Nucleon Momentum and Density Distributions in Nuclei, in, JSTOR, 1991.

[11] A. Ridha, Elastic electron scattering form factors and nuclear momentum distributions in closed and open shell nuclei, in, M. Sc Thesis, University of Baghdad, 2006.

[12] A. Antonov, P. Hodgson, I Zh Petkov Nucleon momentum and density distribution in nuclei, in, London: Oxford University Press, 1988.

[13] A. Antonov, V. Nikolaev, I.Z. Petkov, Nucleon momentum and density distributions of nuclei, Zeitschrift für Physik A Atoms and Nuclei, 297 (1980) 257-260.

[14] W. Reuter, G. Fricke, K. Merle, H. Miska, Nuclear charge distribution and rms radius of C 12 from absolute elastic electron scattering measurements, Physical Review C, 26 (1982) 806.

[15] B.A. Brown, R. Radhi, B.H. Wildenthal, Electric quadrupole and hexadecupole nuclear excitations from the perspectives of electron scattering and modern shell-model theory, Physics Reports, 101 (1983) 313-358.

[16] A. Karpov, A. Denikin, M. Naumenko, A. Alekseev, V. Rachkov, V. Samarin, V. Saiko, V. Zagrebaev, NRV web knowledge base on low-energy nuclear physics, Nuclear Instruments and Methods in Physics Research Section A: Accelerators, Spectrometers, Detectors and Associated Equipment, 859 (2017) 112-124.

[17] Y.-L. Zhao, Z.-Y. Ma, B.-Q. Chen, W.-Q. Shen, Halo structure of nucleus 23 Al, Chinese physics letters, 20 (2003) 53-55.

[18] L. Yu-Jie, L. Yan-Song, Z. Min, L. Zu-Hua, Z. Hong-Yu, Coulomb effects on the formation of proton halo nuclei, Chinese Physics B, 18 (2009) 5267.

[19] B. Chen, Z. Ma, F. Grümmer, S. Krewald, Relativistic mean-field theory study of proton halos in the 2s1d shell, Journal of Physics G: Nuclear and Particle Physics, 24 (1998) 97.

[20] A. Ozawa, T. Suzuki, I. Tanihata, Nuclear size and related topics, Nucl. Phys. A, 693 (2001) 32-62.